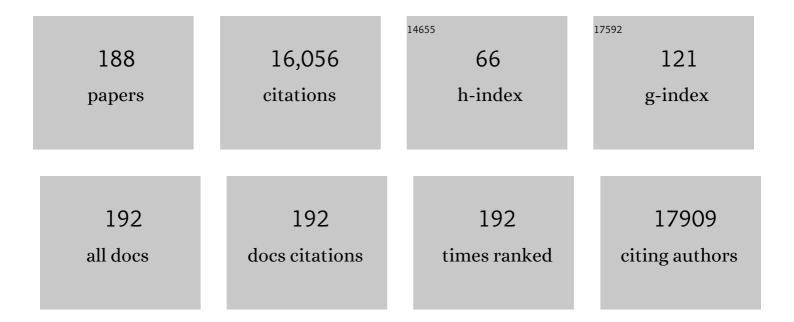


List of Publications by Year in descending order

Source: https://exaly.com/author-pdf/2089068/publications.pdf Version: 2024-02-01



ا ا منا

#	Article	IF	CITATIONS
1	Twinborn TiO ₂ –TiN heterostructures enabling smooth trapping–diffusion–conversion of polysulfides towards ultralong life lithium–sulfur batteries. Energy and Environmental Science, 2017, 10, 1694-1703.	30.8	884
2	Water-evaporation-induced electricity with nanostructured carbon materials. Nature Nanotechnology, 2017, 12, 317-321.	31.5	747
3	Engineering unsymmetrically coordinated Cu-S1N3 single atom sites with enhanced oxygen reduction activity. Nature Communications, 2020, 11, 3049.	12.8	537
4	Capture and Catalytic Conversion of Polysulfides by In Situ Built TiO ₂ â€MXene Heterostructures for Lithium–Sulfur Batteries. Advanced Energy Materials, 2019, 9, 1900219.	19.5	481
5	Robust and Low-Cost Flame-Treated Wood for High-Performance Solar Steam Generation. ACS Applied Materials & Interfaces, 2017, 9, 15052-15057.	8.0	463
6	General synthesis of two-dimensional van der Waals heterostructure arrays. Nature, 2020, 579, 368-374.	27.8	393
7	Solar-driven simultaneous steam production and electricity generation from salinity. Energy and Environmental Science, 2017, 10, 1923-1927.	30.8	380
8	Propelling polysulfides transformation for high-rate and long-life lithium–sulfur batteries. Nano Energy, 2017, 33, 306-312.	16.0	352
9	Manganese Sesquioxide as Cathode Material for Multivalent Zinc Ion Battery with High Capacity and Long Cycle Life. Electrochimica Acta, 2017, 229, 422-428.	5.2	329
10	Superhierarchical Cobaltâ€Embedded Nitrogenâ€Doped Porous Carbon Nanosheets as Twoâ€inâ€One Hosts for Highâ€Performance Lithium–Sulfur Batteries. Advanced Materials, 2018, 30, e1706895.	21.0	300
11	Gassing in Li4Ti5O12-based batteries and its remedy. Scientific Reports, 2012, 2, 913.	3.3	284
12	Allâ€Printed Porous Carbon Film for Electricity Generation from Evaporationâ€Driven Water Flow. Advanced Functional Materials, 2017, 27, 1700551.	14.9	284
13	Rapid mass production of two-dimensional metal oxides and hydroxides via the molten salts method. Nature Communications, 2017, 8, 15630.	12.8	258
14	Cation vacancy stabilization of single-atomic-site Pt1/Ni(OH)x catalyst for diboration of alkynes and alkenes. Nature Communications, 2018, 9, 1002.	12.8	255
15	Aqueous thermogalvanic cells with a high Seebeck coefficient for low-grade heat harvest. Nature Communications, 2018, 9, 5146.	12.8	255
16	Tunable Structural, Electronic, and Optical Properties of Layered Two-Dimensional C ₂ N and MoS ₂ van der Waals Heterostructure as Photovoltaic Material. Journal of Physical Chemistry C, 2017, 121, 3654-3660.	3.1	233
17	Nickel–Copper Alloy Encapsulated in Graphitic Carbon Shells as Electrocatalysts for Hydrogen Evolution Reaction. Advanced Energy Materials, 2018, 8, 1701759.	19.5	225
18	Edgeâ€Rich Feâ^'N ₄ Active Sites in Defective Carbon for Oxygen Reduction Catalysis. Advanced Materials, 2020, 32, e2000966.	21.0	215

#	Article	IF	CITATIONS
19	Efficient strain modulation of 2D materials via polymer encapsulation. Nature Communications, 2020, 11, 1151.	12.8	215
20	Van der Waals epitaxial growth of air-stable CrSe2 nanosheets with thickness-tunable magnetic order. Nature Materials, 2021, 20, 818-825.	27.5	206
21	Oxygenâ€Functionalized Ultrathin Ti ₃ C ₂ T _{<i>x</i>} MXene for Enhanced Electrocatalytic Hydrogen Evolution. ChemSusChem, 2019, 12, 1368-1373.	6.8	204
22	Allâ€Solidâ€State Fiber Supercapacitors with Ultrahigh Volumetric Energy Density and Outstanding Flexibility. Advanced Energy Materials, 2019, 9, 1802753.	19.5	197
23	Synthesis of Ultrathin Metallic MTe ₂ (M = V, Nb, Ta) Single rystalline Nanoplates. Advanced Materials, 2018, 30, e1801043.	21.0	183
24	High-Resolution Scanning Tunneling Spectroscopy of Magnetic Impurity Induced Bound States in the Superconducting Gap of Pb Thin Films. Physical Review Letters, 2008, 100, 226801.	7.8	182
25	Induced Potential in Porous Carbon Films through Water Vapor Absorption. Angewandte Chemie - International Edition, 2016, 55, 8003-8007.	13.8	170
26	A robust strategy for crafting monodisperse Li4Ti5O12 nanospheres as superior rate anode for lithium ion batteries. Nano Energy, 2016, 21, 133-144.	16.0	168
27	Stable Zinc Anodes Enabled by a Zincophilic Polyanionic Hydrogel Layer. Advanced Materials, 2022, 34, e2202382.	21.0	168
28	High-order superlattices by rolling up van der Waals heterostructures. Nature, 2021, 591, 385-390.	27.8	163
29	DNA biosensor based on chitosan film doped with carbon nanotubes. Analytical Biochemistry, 2005, 346, 107-114.	2.4	161
30	Direct Growth of Carbon Nanotubes Doped with Single Atomic Fe–N ₄ Active Sites and Neighboring Graphitic Nitrogen for Efficient and Stable Oxygen Reduction Electrocatalysis. Advanced Functional Materials, 2019, 29, 1906174.	14.9	159
31	Oxygen- and Nitrogen-Enriched 3D Porous Carbon for Supercapacitors of High Volumetric Capacity. ACS Applied Materials & Interfaces, 2015, 7, 24622-24628.	8.0	156
32	How Nitrogen-Doped Graphene Quantum Dots Catalyze Electroreduction of CO ₂ to Hydrocarbons and Oxygenates. ACS Catalysis, 2017, 7, 6245-6250.	11.2	129
33	Enhanced Sulfur Redox and Polysulfide Regulation via Porous VN-Modified Separator for Li–S Batteries. ACS Applied Materials & Interfaces, 2019, 11, 5687-5694.	8.0	126
34	Secondary batteries with multivalent ions for energy storage. Scientific Reports, 2015, 5, 14120.	3.3	125
35	Reversible and selective ion intercalation through the top surface of few-layer MoS2. Nature Communications, 2018, 9, 5289.	12.8	119
36	Synthetic Control of Two-Dimensional NiTe ₂ Single Crystals with Highly Uniform Thickness Distributions. Journal of the American Chemical Society, 2018, 140, 14217-14223.	13.7	119

#	Article	IF	CITATIONS
37	A Lightweight 3D Cu Nanowire Network with Phosphidation Gradient as Current Collector for Highâ€Đensity Nucleation and Stable Deposition of Lithium. Advanced Materials, 2019, 31, e1904991.	21.0	114
38	Thermal–Electric Nanogenerator Based on the Electrokinetic Effect in Porous Carbon Film. Advanced Energy Materials, 2018, 8, 1702481.	19.5	111
39	Unveiling the Axial Hydroxyl Ligand on FeN ₄ C Electrocatalysts and Its Impact on the pHâ€Dependent Oxygen Reduction Activities and Poisoning Kinetics. Advanced Science, 2020, 7, 2000176.	11.2	111
40	2D Metallic Transitionâ€Metal Dichalcogenides: Structures, Synthesis, Properties, and Applications. Advanced Functional Materials, 2021, 31, 2105132.	14.9	111
41	Dual-Mode Electronic Skin with Integrated Tactile Sensing and Visualized Injury Warning. ACS Applied Materials & Interfaces, 2017, 9, 37493-37500.	8.0	110
42	Highly Efficient Water Harvesting with Optimized Solar Thermal Membrane Distillation Device. Global Challenges, 2018, 2, 1800001.	3.6	108
43	Alkali-Metal-Doped B80 as High-Capacity Hydrogen Storage Media. Journal of Physical Chemistry C, 2008, 112, 19268-19271.	3.1	107
44	Reviving catalytic activity of nitrides by the doping of the inert surface layer to promote polysulfide conversion in lithium-sulfur batteries. Nano Energy, 2019, 60, 305-311.	16.0	106
45	Atmosphericâ€Pressure Synthesis of 2D Nitrogenâ€Rich Tungsten Nitride. Advanced Materials, 2018, 30, e1805655.	21.0	104
46	Carbon Nanotubes-Based Amperometric Cholesterol Biosensor Fabricated Through Layer-by-Layer Technique. Electroanalysis, 2004, 16, 1992-1998.	2.9	101
47	van der Waals Epitaxial Growth of Atomically Thin 2D Metals on Danglingâ€Bondâ€Free WSe ₂ and WS ₂ . Advanced Functional Materials, 2019, 29, 1806611.	14.9	99
48	Adsorption of DNA/RNA nucleobases on hexagonal boron nitride sheet: an ab initio study. Physical Chemistry Chemical Physics, 2011, 13, 12225.	2.8	96
49	Revealing the Active Species for Aerobic Alcohol Oxidation by Using Uniform Supported Palladium Catalysts. Angewandte Chemie - International Edition, 2018, 57, 4642-4646.	13.8	93
50	Flexible supercapacitors. Particuology, 2013, 11, 371-377.	3.6	92
51	Thermal conductivity of electrospinning chain-aligned polyethylene oxide (PEO). Polymer, 2017, 115, 52-59.	3.8	92
52	Experimental and theoretical studies of effective thermal conductivity of composites made of silicone rubber and Al2O3 particles. Thermochimica Acta, 2015, 614, 1-8.	2.7	91
53	Oxidation State Modulation of Bismuth for Efficient Electrocatalytic Nitrogen Reduction to Ammonia. Advanced Functional Materials, 2021, 31, 2100300.	14.9	90
54	P-N conversion in thermogalvanic cells induced by thermo-sensitive nanogels for body heat harvesting. Nano Energy, 2019, 57, 473-479.	16.0	89

#	Article	IF	CITATIONS
55	Theoretical Investigation of the Intercalation Chemistry of Lithium/Sodium Ions in Transition Metal Dichalcogenides. Journal of Physical Chemistry C, 2017, 121, 13599-13605.	3.1	87
56	Microscopic origin of the <mml:math xmlns:mml="http://www.w3.org/1998/Math/MathML"><mml:mi>p</mml:mi>-type conductivity of the topological crystalline insulator SnTe and the effect of Pb alloying. Physical Review B, 2014, 89, .</mml:math 	3.2	84
57	Highâ€Performance Hazy Silver Nanowire Transparent Electrodes through Diameter Tailoring for Semitransparent Photovoltaics. Advanced Functional Materials, 2018, 28, 1705409.	14.9	84
58	Flexible Pseudocapacitive Electrochromics via Inkjet Printing of Additiveâ€Free Tungsten Oxide Nanocrystal Ink. Advanced Energy Materials, 2020, 10, 2000142.	19.5	82
59	Magnetism of C Adatoms on BN Nanostructures: Implications for Functional Nanodevices. Journal of the American Chemical Society, 2009, 131, 1796-1801.	13.7	80
60	The transition metal surface dependent methane decomposition in graphene chemical vapor deposition growth. Nanoscale, 2017, 9, 11584-11589.	5.6	76
61	Probing the Oxygen Reduction Reaction Intermediates and Dynamic Active Site Structures of Molecular and Pyrolyzed Fe–N–C Electrocatalysts by In Situ Raman Spectroscopy. ACS Catalysis, 2022, 12, 7811-7820.	11.2	76
62	Ultra-stretchable, bio-inspired ionic skins that work stably in various harsh environments. Journal of Materials Chemistry A, 2018, 6, 24114-24119.	10.3	75
63	Fractal dendrite-based electrically conductive composites for laser-scribed flexible circuits. Nature Communications, 2015, 6, 8150.	12.8	73
64	Experimental Evidence of Chiral Symmetry Breaking in Kekulé-Ordered Graphene. Physical Review Letters, 2021, 126, 206804.	7.8	72
65	Universal Descriptor for Large-Scale Screening of High-Performance MXene-Based Materials for Energy Storage and Conversion. Chemistry of Materials, 2018, 30, 2687-2693.	6.7	71
66	Density functional theory calculations: A powerful tool to simulate and design high-performance energy storage and conversion materials. Progress in Natural Science: Materials International, 2019, 29, 247-255.	4.4	70
67	Hierarchical SnS/SnS2 heterostructures grown on carbon cloth as binder-free anode for superior sodium-ion storage. Carbon, 2019, 148, 525-531.	10.3	70
68	An organic nickel salt-based electrolyte additive boosts homogeneous catalysis for lithium-sulfur batteries. Energy Storage Materials, 2020, 33, 290-297.	18.0	69
69	Fabricating polyoxometalates-stabilized single-atom site catalysts in confined space with enhanced activity for alkynes diboration. Nature Communications, 2021, 12, 4205.	12.8	69
70	Unusual High Oxygen Reduction Performance in All-Carbon Electrocatalysts. Scientific Reports, 2014, 4, 6289.	3.3	67
71	Spontaneous self-intercalation of copper atoms into transition metal dichalcogenides. Science Advances, 2020, 6, eaay4092.	10.3	67
72	Ultrafast growth of large single crystals of monolayer WS2 and WSe2. National Science Review, 2020, 7, 737-744.	9.5	64

#	Article	IF	CITATIONS
73	Polymer composites with enhanced thermal conductivity via oriented boron nitride and alumina hybrid fillers assisted by 3-D printing. Ceramics International, 2020, 46, 20810-20818.	4.8	64
74	Direct van der Waals epitaxial growth of 1D/2D Sb2Se3/WS2 mixed-dimensional p-n heterojunctions. Nano Research, 2019, 12, 1139-1145.	10.4	63
75	<i>In Situ</i> X-ray Absorption Spectroscopic Investigation of the Capacity Degradation Mechanism in Mg/S Batteries. Nano Letters, 2019, 19, 2928-2934.	9.1	63
76	Ultrafast self-heating synthesis of robust heterogeneous nanocarbides for high current density hydrogen evolution reaction. Nature Communications, 2022, 13, .	12.8	62
77	Controllable synthesis of NiS and NiS2 nanoplates by chemical vapor deposition. Nano Research, 2020, 13, 2506-2511.	10.4	61
78	Growth of Single-Crystalline Cadmium Iodide Nanoplates, CdI ₂ /MoS ₂ (WS ₂ , WSe ₂) van der Waals Heterostructures, and Patterned Arrays. ACS Nano, 2017, 11, 3413-3419.	14.6	59
79	Synthesis of 2D Layered Bil ₃ Nanoplates, Bil ₃ /WSe ₂ van der Waals Heterostructures and Their Electronic, Optoelectronic Properties. Small, 2017, 13, 1701034.	10.0	59
80	Endoepitaxial growth of monolayer mosaic heterostructures. Nature Nanotechnology, 2022, 17, 493-499.	31.5	58
81	Molecular and atomic adsorption of hydrogen on <mml:math xmlns:mml="http://www.w3.org/1998/Math/MathML" altimg="si14.gif" display="inline" overflow="scroll"><mml:mrow><mml:msub><mml:mrow><mml:mtext>TiO</mml:mtext></mml:mrow><mml:n nanotubes: An ab initio study. Chemical Physics Letters. 2009. 475. 82-85.</mml:n </mml:msub></mml:mrow></mml:math 	ırov 7 36 mm	ll:mf7>2
82	Atomic palladium on graphitic carbon nitride as a hydrogen evolution catalyst under visible light irradiation. Communications Chemistry, 2019, 2, .	4.5	57
83	Unraveling the solvent induced welding of silver nanowires for high performance flexible transparent electrodes. Nanoscale, 2018, 10, 12981-12990.	5.6	55
84	Mo ₂ C-MoO ₂ Heterostructure Quantum Dots for Enhanced Electrocatalytic Nitrogen Reduction to Ammonia. ACS Nano, 2022, 16, 643-654.	14.6	55
85	Nickeloceneâ€Precursorâ€Facilitated Fast Growth of Graphene/hâ€BN Vertical Heterostructures and Its Applications in OLEDs. Advanced Materials, 2017, 29, 1701325.	21.0	54
86	LiNi0.8Co0.15Al0.05O2 as both a trapper and accelerator of polysulfides for lithium-sulfur batteries. Energy Storage Materials, 2019, 17, 111-117.	18.0	54
87	Dirac Fermions in Strongly Bound Graphene Systems. Physical Review Letters, 2012, 109, 206802.	7.8	53
88	Phaseâ€Tunable Synthesis of Ultrathin Layered Tetragonal CoSe and Nonlayered Hexagonal CoSe Nanoplates. Advanced Materials, 2019, 31, e1900901.	21.0	52
89	Theory of the Dirac half metal and quantum anomalous Hall effect in Mn-intercalated epitaxial graphene. Physical Review B, 2015, 92, .	3.2	50
90	Flexible microfluidics nanogenerator based on the electrokinetic conversion. Nano Energy, 2016, 30, 684-690.	16.0	50

#	Article	IF	CITATIONS
91	Improving a Mg/S Battery with YCl ₃ Additive and Magnesium Polysulfide. Advanced Science, 2019, 6, 1800981.	11.2	50
92	Regulating the Li2S deposition by grain boundaries in metal nitrides for stable lithium-sulfur batteries. Nano Energy, 2022, 91, 106669.	16.0	49
93	A dual-carbon-anchoring strategy to fabricate flexible LiMn2O4 cathode for advanced lithium-ion batteries with high areal capacity. Nano Energy, 2020, 67, 104256.	16.0	46
94	Vapor phase growth of two-dimensional PdSe2 nanosheets for high-photoresponsivity near-infrared photodetectors. Nano Research, 2020, 13, 2091-2097.	10.4	44
95	xmlns:mml="http://www.w3.org/1998/Math/MathML" display="inline"> <mml:mrow><mml:mrow><mml:mo>(</mml:mo><mml:mrow><mml:mn>2</mml:mn><mml:mov< td=""><td>ver) Tj ETQ 3.2</td><td>1911 1 0.784</td></mml:mov<></mml:mrow></mml:mrow></mml:mrow>	ver) Tj ETQ 3.2	1911 1 0.784
96	High areal specific capacity of Ni ₃ V ₂ O ₈ /carbon cloth hierarchical structures as flexible anodes for sodium-ion batteries. Journal of Materials Chemistry A, 2017, 5, 15517-15524.	10.3	43
97	Coordination Engineering in Cobalt–Nitrogen-Functionalized Materials for CO ₂ Reduction. Journal of Physical Chemistry Letters, 2019, 10, 6551-6557.	4.6	42
98	Printed Zinc Paper Batteries. Advanced Science, 2022, 9, e2103894.	11.2	42
99	Spontaneous edge-defect formation and defect-induced conductance suppression in graphene nanoribbons. Physical Review B, 2010, 82, .	3.2	41
100	Effects of solvent on structures and properties of electrospun poly(ethylene oxide) nanofibers. Journal of Applied Polymer Science, 2018, 135, 45787.	2.6	40
101	Liquid electrolyte immobilized in compact polymer matrix for stable sodium metal anodes. Energy Storage Materials, 2019, 23, 610-616.	18.0	40
102	Electrochemical Study of Breast Cancer Cells MCF-7 and Its Application in Evaluating the Effect of Diosgenin. Analytical Sciences, 2005, 21, 561-564.	1.6	39
103	Group VB transition metal dichalcogenides for oxygen reduction reaction and strain-enhanced activity governed by p-orbital electrons of chalcogen. Nano Research, 2019, 12, 925-930.	10.4	39
104	Chargeâ€Gradient Hydrogels Enable Direct Zero Liquid Discharge for Hypersaline Wastewater Management. Advanced Materials, 2021, 33, e2100141.	21.0	37
105	Phase Engineering of Atomically Thin Perovskite Oxide for Highly Active Oxygen Evolution. Advanced Functional Materials, 2021, 31, 2102002.	14.9	37
106	Effects of strain and oxygen vacancies on the ferroelectric and antiferrodistortive distortions in <mml:math xmlns:mml="http://www.w3.org/1998/Math/MathML"><mml:mrow><mml:msub><mml:mi>PbTiO</mml:mi><mml: Physical Review B, 2015, 92, .</mml: </mml:msub></mml:mrow></mml:math 	l:mn>3 <td>പണ്:mn> </td>	പ ണ്: mn>
107	Atomic Imaging of Subsurface Interstitial Hydrogen and Insights into Surface Reactivity of Palladium	13.8	36
108	Theoretical Investigation of the Electrochemical Performance of Transition Metal Nitrides for Lithium–Sulfur Batteries. Journal of Physical Chemistry C, 2019, 123, 25025-25030.	3.1	35

#	Article	IF	CITATIONS
109	Synthesis of ultrathin two-dimensional nanosheets and van der Waals heterostructures from non-layered γ-Cul. Npj 2D Materials and Applications, 2018, 2, .	7.9	34
110	Lithium Intercalation Induced Decoupling of Epitaxial Graphene on SiC(0001): Electronic Property and Dynamic Process. Journal of Physical Chemistry C, 2011, 115, 23992-23997.	3.1	32
111	Selfâ€Powered Multimodal Temperature and Force Sensor Basedâ€On a Liquid Droplet. Angewandte Chemie - International Edition, 2016, 55, 15864-15868.	13.8	32
112	High-performance asymmetric electrodes photodiode based on Sb/WSe2 heterostructure. Nano Research, 2019, 12, 339-344.	10.4	32
113	Enhanced thermal conductivity of alumina and carbon fibre filled composites by 3-D printing. Thermochimica Acta, 2020, 690, 178649.	2.7	32
114	van der Waals epitaxial growth of ultrathin metallic NiSe nanosheets on WSe2 as high performance contacts for WSe2 transistors. Nano Research, 2019, 12, 1683-1689.	10.4	31
115	Synthesis of Ultrathin 2D Nonlayered αâ€MnSe Nanosheets, MnSe/WS ₂ Heterojunction for Highâ€Performance Photodetectors. Small Structures, 2021, 2, 2100028.	12.0	31
116	Degradation and regeneration of Fe–N _{<i>x</i>} active sites for the oxygen reduction reaction: the role of surface oxidation, Fe demetallation and local carbon microporosity. Chemical Science, 2021, 12, 11576-11584.	7.4	30
117	In Situ Electrochemically Derived Amorphousâ€Li ₂ S for High Performance Li ₂ S/Graphite Full Cell. Small, 2018, 14, e1703871.	10.0	29
118	Electrokinetic Supercapacitor for Simultaneous Harvesting and Storage of Mechanical Energy. ACS Applied Materials & Interfaces, 2018, 10, 8010-8015.	8.0	29
119	Narrowed bandgaps and stronger excitonic effects from small boron nitride nanotubes. Chemical Physics Letters, 2009, 476, 240-243.	2.6	28
120	Abundant grain boundaries activate highly efficient lithium ion transportation in high rate Li4Ti5O12 compact microspheres. Journal of Materials Chemistry A, 2019, 7, 1168-1176.	10.3	28
121	High areal capacity flexible sulfur cathode based on multi-functionalized super-aligned carbon nanotubes. Nano Research, 2019, 12, 1105-1113.	10.4	28
122	Selective adsorption of first-row atoms on BN nanotubes. Chemical Physics Letters, 2006, 426, 148-154.	2.6	27
123	Few-layer Ti3C2T MXene delaminated via flash freezing for high-rate electrochemical capacitive energy storage. Journal of Energy Chemistry, 2020, 48, 233-240.	12.9	27
124	Flexible and free-standing hetero-electrocatalyst of high-valence-cation doped MoS ₂ /MoO ₂ /CNT foam with synergistically enhanced hydrogen evolution reaction catalytic activity. Journal of Materials Chemistry A, 2020, 8, 14944-14954.	10.3	25
125	Mitigating Metal Dissolution and Redeposition of Pt-Co Catalysts in PEM Fuel Cells: Impacts of Structural Ordering and Particle Size. Journal of the Electrochemical Society, 2020, 167, 064520.	2.9	25
126	Strainâ€Plasmonic Coupled Broadband Photodetector Based on Monolayer MoS ₂ . Small, 2022, 18, e2107104.	10.0	25

#	Article	IF	CITATIONS
127	Comprehensive approaches to three-dimensional flexible supercapacitor electrodes based on MnO2/carbon nanotube/activated carbon fiber felt. Journal of Materials Science, 2017, 52, 5788-5798.	3.7	24
128	Tailoring Native Defects and Zinc Impurities in Li ₄ Ti ₅ O ₁₂ : Insights from First-Principles Study. Journal of Physical Chemistry C, 2015, 119, 5238-5245.	3.1	23
129	Enhanced thermal conductivity by combined fillers in polymer composites. Thermochimica Acta, 2019, 676, 198-204.	2.7	23
130	RuO2 clusters derived from bulk SrRuO3: Robust catalyst for oxygen evolution reaction in acid. Nano Research, 2022, 15, 1959-1965.	10.4	23
131	Controlled Synthesis of Ultrathin PtSe ₂ Nanosheets with Thicknessâ€Tunable Electrical and Magnetoelectrical Properties. Advanced Science, 2022, 9, e2103507.	11.2	23
132	Layered MXene Protected Lithium Metal Anode as an Efficient Polysulfide Blocker for Lithium‧ulfur Batteries. Batteries and Supercaps, 2020, 3, 892-899.	4.7	22
133	Modulating Surface Composition and Oxygen Reduction Reaction Activities of Pt–Ni Octahedral Nanoparticles by Microwave-Enhanced Surface Diffusion during Solvothermal Synthesis. Chemistry of Materials, 2018, 30, 4355-4360.	6.7	21
134	Inâ€plane epitaxial growth of 2D CoSeâ€WSe 2 metalâ€semiconductor lateral heterostructures with improved WSe 2 transistors performance. InformaÄnÃ-Materiály, 2021, 3, 222-228.	17.3	21
135	Femtomolarâ€Level Molecular Sensing of Monolayer Tungsten Diselenide Induced by Heteroatom Doping with Longâ€Term Stability. Advanced Functional Materials, 2022, 32, .	14.9	21
136	Unraveling the Influence of Metal Substrates on Graphene Nucleation from First-Principles Study. Journal of Physical Chemistry C, 2016, 120, 23239-23245.	3.1	20
137	Boosting the Efficient Energy Output of Electret Nanogenerators by Suppressing Air Breakdown under Ambient Conditions. ACS Applied Materials & Interfaces, 2019, 11, 3984-3989.	8.0	20
138	Plasma-etched functionalized graphene as a metal-free electrode catalyst in solid acid fuel cells. Journal of Materials Chemistry A, 2020, 8, 2445-2452.	10.3	20
139	Ultrasensitive molecular sensing of few-layer niobium diselenide. Journal of Materials Chemistry A, 2021, 9, 2725-2733.	10.3	20
140	Highly Selective Synthesis of Monolayer or Bilayer WSe ₂ Single Crystals by Pre-annealing the Solid Precursor. Chemistry of Materials, 2021, 33, 1307-1313.	6.7	20
141	Room-temperature dissociative hydrogen chemisorption on boron-doped fullerenes. Physical Review B, 2008, 77, .	3.2	19
142	Ab initio Study of Half-Metallicity and Magnetism of Complex Organometallic Molecular Wires. Journal of Physical Chemistry C, 2011, 115, 7292-7297.	3.1	19
143	Ferromagnetism and topological surface states of manganese doped Bi2Te3: Insights from density-functional calculations. Journal of Chemical Physics, 2014, 140, 124704.	3.0	19
144	All-Day Thermogalvanic Cells for Environmental Thermal Energy Harvesting. Research, 2019, 2019, 2460953.	5.7	18

#	Article	IF	CITATIONS
145	Coexistence of extended flat band and Kekulé order in Li-intercalated graphene. Physical Review B, 2022, 105, .	3.2	18
146	Synthesis of Group VIII Magnetic Transition-Metal-Doped Monolayer MoSe ₂ . ACS Nano, 2022, 16, 10623-10631.	14.6	18
147	Pt Submonolayers on Au Nanoparticles: Coverage-Dependent Atomic Structures and Electrocatalytic Stability on Methanol Oxidation. Journal of Physical Chemistry C, 2016, 120, 28664-28671.	3.1	17
148	Heat-triggered high-performance thermocells enable a self-powered forest fire alarm. Journal of Materials Chemistry A, 2021, 9, 26119-26126.	10.3	17
149	Realizing Ultralow Concentration Gelation of Graphene Oxide with Artificial Interfaces. Advanced Materials, 2019, 31, e1805075.	21.0	16
150	Solubility-Dependent Protective Effects of Binary Alloys for Lithium Anode. ACS Applied Energy Materials, 2020, 3, 2278-2284.	5.1	16
151	High-efficiency solar heat storage enabled by adaptive radiation management. Cell Reports Physical Science, 2021, 2, 100533.	5.6	15
152	Controllable Preparation of 2D Vertical van der Waals Heterostructures and Superlattices for Functional Applications. Small, 2022, 18, e2107059.	10.0	15
153	Synergistic effect of carbon fiber and alumina in improving the thermal conductivity of polydimethylsiloxane composite. Thermochimica Acta, 2021, 703, 178980.	2.7	14
154	Prediction of interfacial thermal resistance of carbon fiber in one dimensional fiber-reinforced composites using laser flash analysis. Composites Science and Technology, 2015, 110, 69-75.	7.8	13
155	Vertically aligned carbon nanotubes grown on reduced graphene oxide as high-performance thermal interface materials. Journal of Materials Science, 2020, 55, 9414-9424.	3.7	13
156	Nondegenerate Pâ€Type Inâ€Doped SnS ₂ Monolayer Transistor. Advanced Electronic Materials, 2021, 7, 2001168.	5.1	13
157	Highâ€Resolution Van der Waals Stencil Lithography for 2DÂTransistors. Small, 2021, 17, e2101209.	10.0	13
158	Ultimate dielectric scaling of 2D transistors via van der Waals metal integration. Nano Research, 2022, 15, 1603-1608.	10.4	13
159	Monolayer charge-neutral graphene on platinum with extremely weak electron-phonon coupling. Physical Review B, 2015, 92, .	3.2	12
160	Origin of storage capacity enhancement by replacing univalent ion with multivalent ion for energy storage. Electrochimica Acta, 2018, 282, 30-37.	5.2	11
161	Thermal design and optimization of lithium ion batteries for unmanned aerial vehicles. Energy Storage, 2019, 1, e48.	4.3	10
162	Two-dimensional intrinsic ferromagnetic monolayer transition metal oxyhydroxide. Physical Review B, 2021, 103, .	3.2	10

#	Article	IF	CITATIONS
163	Promoting the optoelectronic and ferromagnetic properties of Cr2S3 nanosheets via Se doping. Science China: Physics, Mechanics and Astronomy, 2022, 65, .	5.1	10
164	Metallicity retained by covalent functionalization of graphene with phenyl groups. Nanoscale, 2013, 5, 7537.	5.6	9
165	Selective growth of wide band gap atomically thin Sb2O3 inorganic molecular crystal on WS2. Nano Research, 2019, 12, 2781-2787.	10.4	9
166	Reversible function switching of Ag catalyst in Mg/S battery with chloride-containing electrolyte. Energy Storage Materials, 2021, 42, 513-516.	18.0	9
167	Ferromagnetism with in-plane magnetization, Dirac spin-gapless semiconducting properties, and tunable topological states in two-dimensional rare-earth metal dinitrides. Physical Review B, 2022, 105,	3.2	9
168	A first-principles study of lithium and sodium storage in two-dimensional graphitic carbon nitride. New Carbon Materials, 2018, 33, 510-515.	6.1	8
169	Activated dissociation ofO2on Pb(111) surfaces by Pb adatoms. Physical Review B, 2009, 80, .	3.2	7
170	Ab Initio Investigation about the Possibility of Ferromagnetism Induced by Boron Vacancy in BN Nanotubes. Journal of Physical Chemistry C, 2010, 114, 4357-4361.	3.1	7
171	Formation, Morphology, and Effect of Complex Defects in Boron Nitride Nanotubes: An ab initio Calculation. Journal of Physical Chemistry C, 2011, 115, 12782-12788.	3.1	7
172	Freezeâ€drying method prepared <scp>UHMWPE/CNT</scp> s composites with optimized micromorphologies and improved tribological performance. Journal of Applied Polymer Science, 2015, 132, .	2.6	7
173	First principles study of ruthenium(<scp>ii</scp>) sensitizer adsorption on anatase TiO ₂ (001) surface. RSC Advances, 2015, 5, 60230-60236.	3.6	7
174	Manipulation of the Electronic State of Mott Iridate Superlattice through Protonation Induced Electronâ€Filling. Advanced Functional Materials, 2021, 31, 2100261.	14.9	7
175	Stimulating the Pre-Catalyst Redox Reaction and the Proton–Electron Transfer Process of Cobalt Phthalocyanine for CO ₂ Electroreduction. Journal of Physical Chemistry C, 2022, 126, 9665-9672.	3.1	7
176	Long periodic oscillation of electronic properties in capped finite-length armchair carbon nanotubes. Physical Review B, 2005, 71, .	3.2	6
177	First-principles study of native defects in LiTi2O4. Computational Materials Science, 2015, 96, 263-267.	3.0	6
178	Preparing spin-polarized scanning tunneling microscope probes on capped carbon nanotubes by Fe doping: A first-principles study. Applied Physics Letters, 2009, 94, 193106.	3.3	4
179	TUNABLE ELECTRIC CONDUCTIVITIES OF Au -DOPED BORON NITRIDE NANOTUBES. Nano, 2007, 02, 367-372.	1.0	3
180	Feâ€Nâ€C Catalysts: Direct Growth of Carbon Nanotubes Doped with Single Atomic Fe–N ₄ Active Sites and Neighboring Graphitic Nitrogen for Efficient and Stable Oxygen Reduction Electrocatalysis (Adv. Funct. Mater. 49/2019). Advanced Functional Materials, 2019, 29, 1970332.	14.9	3

#	Article	IF	CITATIONS
181	Hollow "graphene―microtubes using polyacrylonitrile nanofiber template and potential applications of field emission. Carbon, 2020, 167, 439-445.	10.3	3
182	LixNa2â^'xW4O13 nanosheet for scalable electrochromic device. Frontiers of Optoelectronics, 2021, 14, 298-310.	3.7	3
183	Tuning the Hydration Entropy of Cations during Electrochemical Intercalation for High Thermopower. Advanced Energy and Sustainability Research, 2022, 3, .	5.8	3
184	Nanoplates: Synthesis of 2D Layered Bil ₃ Nanoplates, Bil ₃ /WSe ₂ van der Waals Heterostructures and Their Electronic, Optoelectronic Properties (Small 38/2017). Small, 2017, 13, .	10.0	2
185	Family of Magicâ€Sized Carbon Clusters on Transition Metal Substrates. Advanced Functional Materials, 2020, 30, 2006671.	14.9	2
186	A dual-regulation strategy of B/N codoped CNT-encapsulated Ni nanoparticles as a catalytic host and separator coating promises high-performance Li-S batteries. Science China Technological Sciences, 2022, 65, 1567-1577.	4.0	2
187	Recent advances in screening two-dimensional materials for high-performance energy storage and conversion devices based on electronic structure theory. Chinese Science Bulletin, 2021, 66, 640-656.	0.7	1
188	Thermal conductivity of graphite nanofibers electrospun from graphene oxide-doped polyimide. New Carbon Materials, 2021, 36, 940-947.	6.1	0